Digital holographic characterization of liquid micro-lenses array fabricated in electrode-less configuration

L. Miccio, V. Vespini, S. Grilli, M. Paturzo, A. Finizio, S. De Nicola, and P. Ferraro*

Istituto Nazionale di Ottica Applicata (CNR-INOA) & Istituto di Cibernetica del CNR "E. Caianiello",

Via Campi Flegrei 34 – 80078 Pozzuoli (NA), Italy

ABSTRACT

We show how thin liquid film on polar dielectric substrate can form an array of liquid micro-lenses. The effect is driven by the pyroelectric effect leading to a new concept in electro-wetting (EW). EW is a viable method for actuation of liquids in microfluidic systems and requires the design and fabrication of complex electrodes for suitable actuation of liquids. When compared to conventional electrowetting devices, the pyroelectric effect allowed to have an electrode-less and circuitless configuration. In our case the surface electric charge induced by the thermal stimulus is able to pattern selectively the surface wettability according to geometry of the ferroelectric domains micro-engineered into the lithium niobate crystal. We show that different geometries of liquid microlenses can be obtained showing also a tuneability of the focal lenses down to 1.6 mm. Thousand of liquid microlenses, each with 100 μm diameter, can be formed and actuated. Also different geometries such as hemi-cylindrical and toroidal liquid structures can be easily obtained.
By means of a digital holography method, an accurate characterization of the micro-lenses curvature is performed and presented. The preliminary results concerning the imaging capability of the micro-lens array are also reported. Microlens array can find application in medical stereo-endoscopy, imaging, telecommunication and optical data storage too.

Keywords: elettrowetting, digital holography, lithium niobate, pyroelectric effect

1. INTRODUCTION

In recent years, researcher developed new technique to fabricate adaptive optical element. In this framework liquid lenses are becoming important optical devices for a wide variety of applications ranging from mobile-phone cameras to biology. The main advantage is that is possible to change the focal length just changing the liquid shape [1-8]. In fact, this can be effectively modified to obtain different radius of curvature and consequently a varying focal length. Two procedures have been invented to change the shape of the liquid mass. The first one is based on hydrostatic and/or pneumatic forces, devices have flexible and elastic membrane that changes liquid shape [9-12]. Different principle is adopted when using the electrowetting (EW) effect [13-18]. In the latter case electric forces instead of pressure force are used. Basically, the electric charges at the liquid-liquid or at the solid-liquid interface modify the interfacial tension, leading to a new shape of the liquid mass. We present a completely new approach demonstrating that is possible to obtain liquid microlenses using an EW process developed without electrode patterning. We will use the expression electrode-less configuration to underline that the substrate was functionalized so that the substrate itself behaves as electrodes [19,20]. The electrodes were built into the crystal, used as substrate, through a micro-engineering process and were activated pyroelectrically by an appropriate temperature variation. In this way we don't need different material to built the substrate and we avoid complex electrode patterning. The crystal employed was a periodically poled polar dielectric crystal (Lithium Niobate LN) it was used as substrate and the formation of sessile microdroplets was driven by the patterned surface charges induced by the pyroelectric effect. Depending on the patterned substrate we are able to fabricate single lens or array of thousand of microlenses. The magnitude order of these devices is about 100 μm. The fundamental physics responsible of the phenomenon leading to the formation of microdroplets was illustrated and investigated in Ref. [19]. In addition, that work presented very preliminary results on the investigation of the possible applications of those microdroplets for the fabrication of liquid microlenses. A complete optical characterization was carried out in Ref. [20] in order to estimate the focal length variation of the microlenses. The optical characterization is performed by means of a Digital Holographic setup. We use this interferometric technique to calculate directly the focal length of the liquid lenses for different temperature and to characterize their optical goodness in terms of optical aberrations. We will show the imaging properties of this kind of lenses.

2. LENS EFFECT OBSERVATION

The lens effect we observe happens when a PPLN crystal covered by a thin liquid film is subject to a temperature variation. To fabricate the PPLN substrate we employ both sides polished and 500 μm thick LN crystals. We periodically poled by standard electric field poling in order to achieve a square array of hexagonal reversed domains. A standard mask lithography process was used to generate the desired resist pattern and the subsequent application of high voltage pulses led to the formation of the reversed domain grating. Figure 1(a) shows the optical microscope image of a typical PPLN sample used for the formation of the liquid microlenses. An oily substances (pentanoic acid) is deposited on the substrate as a thin film of about 100 μm. An appropriate temperature variation of the PPLN substrate generates the pyroelectric effect which causes the formation of uncompensated surface charges able to activate an EW effect.
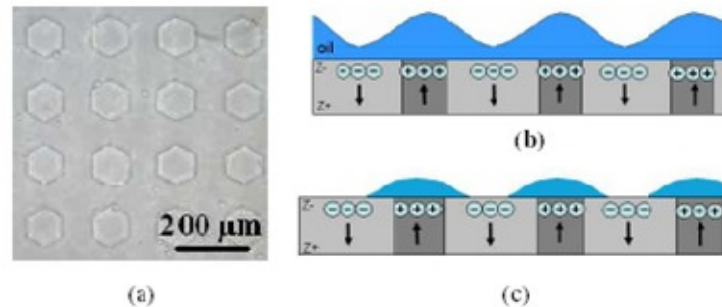

Fig. 1. (a) Optical microscope image of a typical PPLN with a square array of hexagonal reversed domains; (b), (c) schematic views of the sample cross section corresponding to the wave-like lenses regime and to the separated lenses regime of the microlens array, respectively. In both cases the temperature of the substrate is decreasing. The difference between the two regimes stands in the liquid thickness. The black arrows indicate the orientation of the spontaneous polarization.

This phenomenon allows the formation of regular liquid lenses in correspondence of the hexagonal domains. Basically, the heating process makes the spontaneous polarization of the LN crystal to decrease, thus leaving uncompensated charges onto the crystal surface (positive charges in correspondence of the *z-* face and *viceversa*). Conversely, the cooling process makes the polarization to increase thus generating uncompensated polarization charges with opposite signs respect to the heating process (positive charges in correspondence of the *z+* face and *viceversa*). The charge displacement during heating and cooling process is schematically depicted in Fig. 2. While the correspondent electrical field surface distribution and liquid surface tension are showed in Fig.3. We observed two different regimes of the microlens array: Wave like Lens Regime (WLR) and Separated Lens Regime (SLR). Figure 1(b),(c) show the schematic views of the sample cross section under the *WLR* and the *SLR*, respectively. The black arrows indicate the orientation of the spontaneous polarization into the original (light grey) and reversed (dark grey) ferroelectric domains. The case reported in this figure refers to the cooling process, so that uncompensated negative charge is developed in correspondence of the negative side of the spontaneous polarization, and *viceversa*.
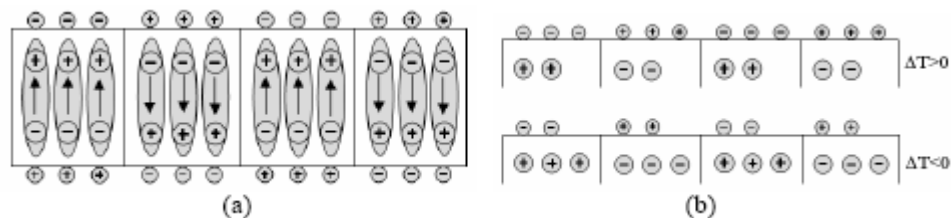

Fig. 2. Schematic view of the PPLN sample cross section with the charge distribution exhibited (a) at the equilibrium state; (b) in case of heating (top) and (bottom) cooling process.
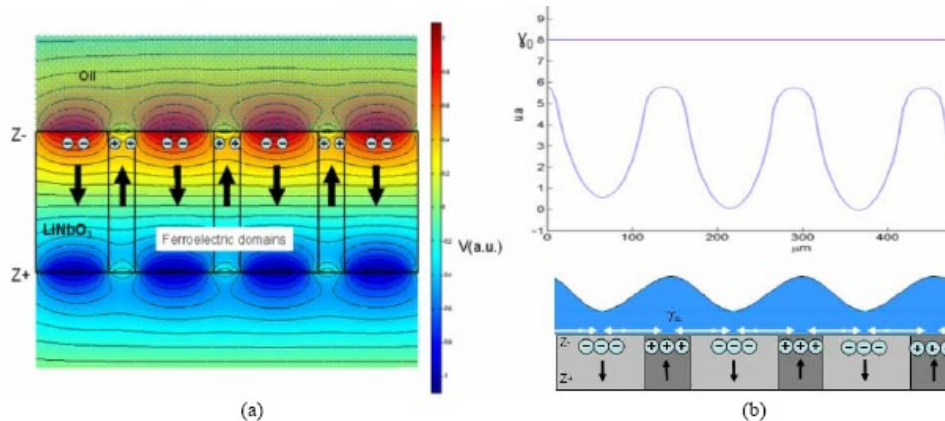
Fig. 3. (a). Schematic view of the sample cross section with the simulated electric potential distribution generated pyroelectrically; (b) (top) surface tension profile and (bottom) the schematic view of the corresponding oil film topography. The black arrows indicate the orientation of the spontaneous polarization.

3. INTERFEROMETRIC ANALYSIS

3.1 Experimental Setup

Both regimes were investigated by an interferometric technique based on a DH microscope set-up, in order to characterize the focusing behaviour and the optical aberrations of the microlenses. Fig. 5 shows the schematic view of the interferometric apparatus used for the measurements. The setup is a Mach Zehnder interferometer. The laser wavelength λ is 532 nm the beam is divided by the beam splitter in the object and reference beams. The first one passes through the sample then it's collected by a lens (L2) and made interfere with the reference beam on a CCD camera used as detector that is positioned out of focus. The interference pattern is named hologram. The sample is placed on a thermo controlled hot plate made of Peltier cell to vary the temperature and an NTC sensor to measure the temperature. The plate is controlled by software that can heat and cool the sample by means of ramps or cycles. We record different hologram for different temperature and calculate the amplitude and phase distribution of the optical wavefield coming from the sample in the image plane of the L2. For each hologram we perform a one-dimensional fitting procedure of the phase distribution to calculate the focal length and a two-dimensional one to evaluate the optical aberration of the lenses in the array.
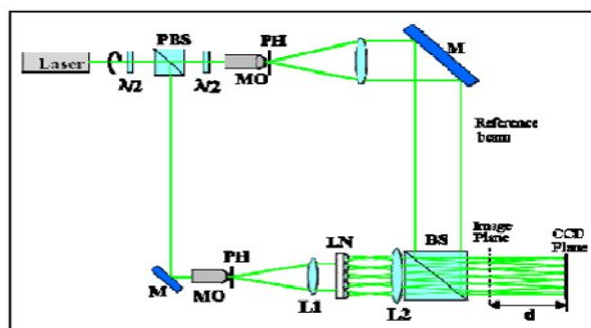

Fig. 4. Schematic view of the interferometric configuration. *PBS* polarizing beam splitter; *MO* microscope objective; *PH* pin-hole; *M* mirror; *BS* beam splitter.

3.2 Results and Discussion

In this section we present the results achieved for the optical characterization of the tunable microlens array under both the WLR and the SLR. In Fig.5 we show two optical microscope image of the lens formation for a very regular array in WLR. Fig.5(a) is recorded before the sample temperature is changed while Fig.5(b) is recorded when the lens formation ends. Fig.5 (d) is the calculated wrapped phase map corresponding to Fig. 5(b) while Fig.5(d) is the unwrapped phase distribution for the same sample.

(a)   (b)

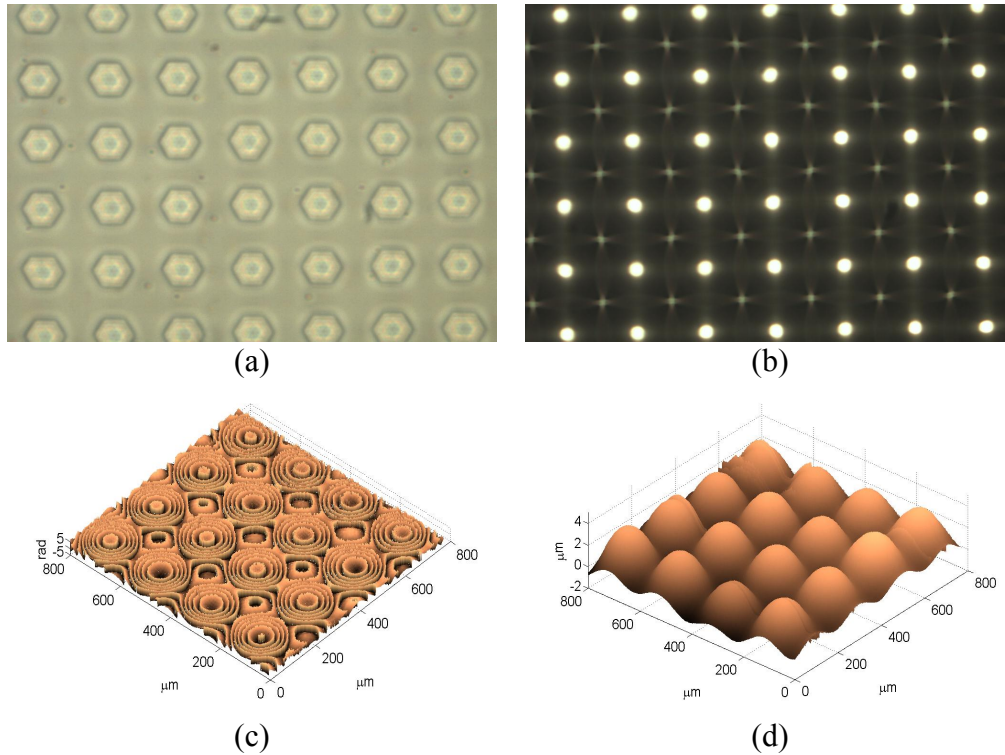(c)   (d)

Fig. 5. Optical microscope images of the oil coated sample (a) before lens effect start and (b) after complete lens formation. Wrapped (c) and unwrapped (d) phase distribution

We perform two different kinds of analysis to evaluate the temperature dependence of the focal length and the optical aberrations of the lenses, thus characterizing both the tunability and the optical performance of the device. The temperature dependence of the focal length was investigated during the cooling and the heating treatments, which were considered as independent processes. It means that the array is heated or cooled by means of temperature ramps. The lenses aberrations were evaluated through a complete analysis of the wavefronts transmitted by the lenses themselves. Fitting procedures are always performed on a single lens of the array and for several lenses. The temperature values range from 30°C to 90°C for both WLR and SLR. Fig. 6 shows the final wrapped phase map distribution for heating and cooling process in the WLR.
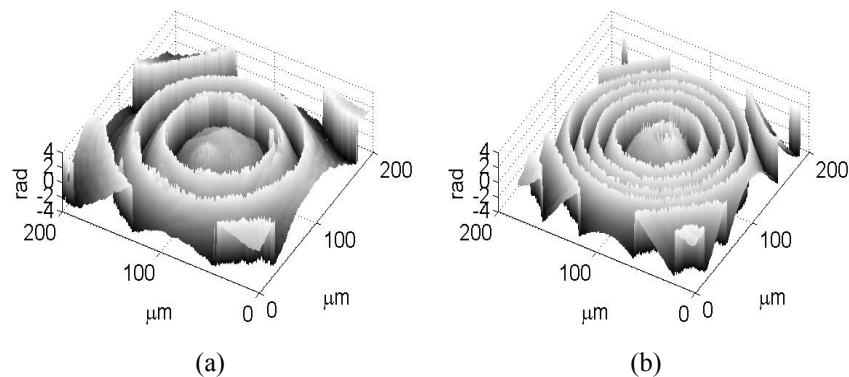

(a)   (b)

Fig. 6 Final wrapped mod 2π phase map during (a) the heating and (b) the cooling process for a single lens of the array.

The lens effect is more pronounced during the cooling where the liquid film on the substrate modify its shape forming lenses with a focal length that ranges from 16mm to 1.5mm. During the whole process the shape continuously changes. Indeed during the heating process the shape of the lenses change when the temperature varies between 30°C and 65°C and then stabilize while temperature is still changing. The focal length variation for the heating process ranges between

9mm and 2.5 mm. Focal length f is calculated from the unwrapped phase $\phi(x,y)$ through a one dimensional fitting process using the following equation:

$$\phi(x) = \frac{\pi}{\lambda}\frac{x^2}{f}$$

The fitted and measured phase value are showed in Fig.7(a) for the heating and Fig.7(b) for the cooling while temperature changing. Fig.7(c) and Fig.7(d) display the correspondent focal length variation in dependence of the temperature.
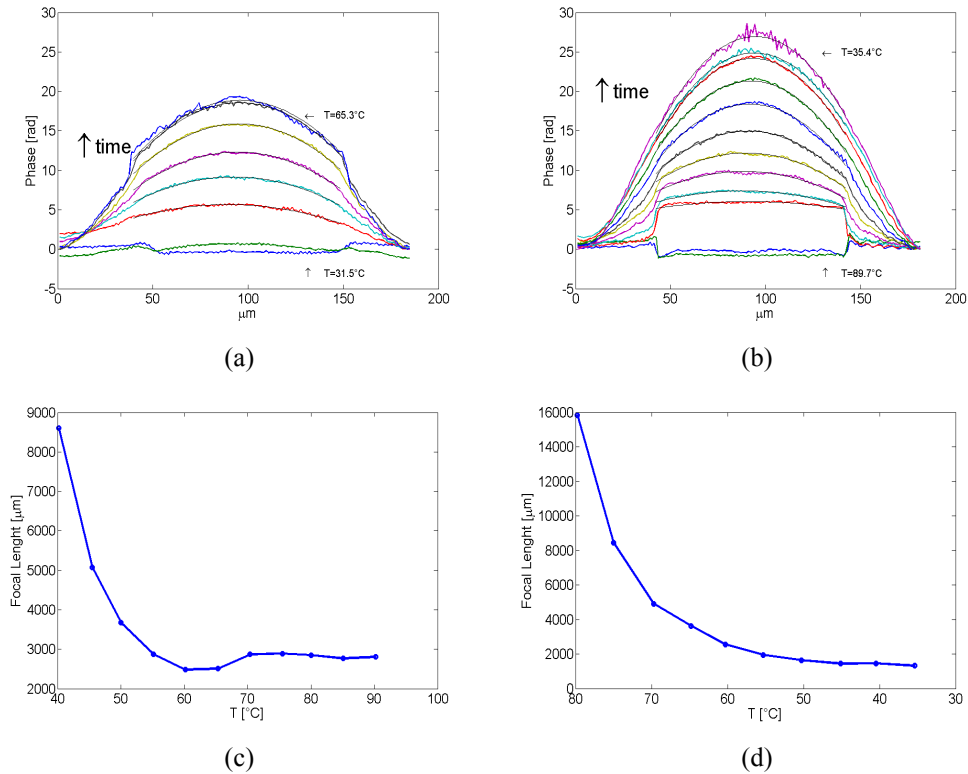

(a)

(b)

(c)

(d)

Fig.7 Experimental and fitted 1D profiles of the unwrapped phase distribution corresponding to (a) the heating and (b) cooling process; (c) (d) focal length variation as a function of temperature in case of the heating and the cooling process, respectively.

The optical behaviour of the microlenses was characterized also in terms of the optical aberrations intrinsically present in the lens array, by applying a two-dimensional fitting procedure. Several holograms of a 4×4 lens array were acquired during the stationary condition, i.e. when the number of fringes is stable in the wrapped phase distribution, while the fitting procedure was performed for each of the three chosen lenses of the array and for the lenses of some arrays at different time instants. The function used for the fitting process is a linear combination of Zernike polynomials. The measured and the calculated phase distribution are presented in Fig. 8(a),(b), respectively. The calculated coefficients show that the phase distribution at the exit of each lens is made of the same terms for each lens and, for each term of the linear expansion, the coefficients of different lenses are similar. This allows us to state that our device displays the same properties for each microlens. Fig. 8(c) displays the focus term, which is the main term contributing to the phase distribution. Figure 6(d) shows the distribution of the third order spherical aberration that appears flat in the central region while diverging in the peripheral one. This divergence is due to the oil layer existing between adjacent lenses, in fact the oil layer redistributes its mass during the temperature variation but, in this case, without breaking up between adjacent lenses. Figure 6(e),(f),(g),(h) show the distributions of the astigmatism terms.
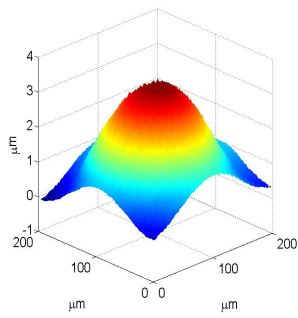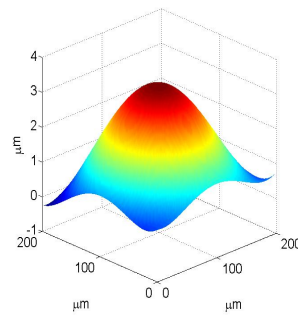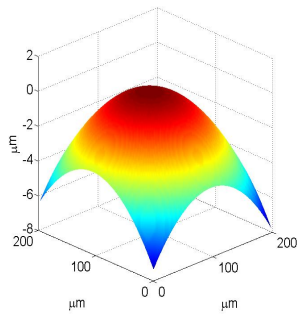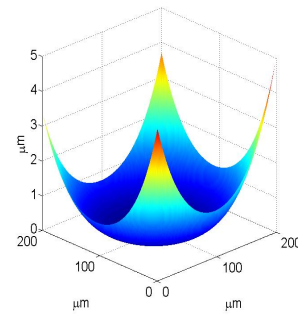
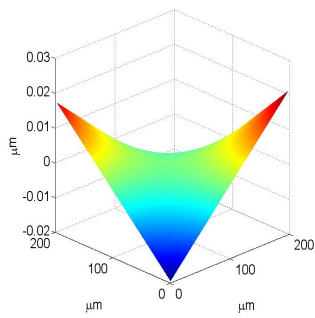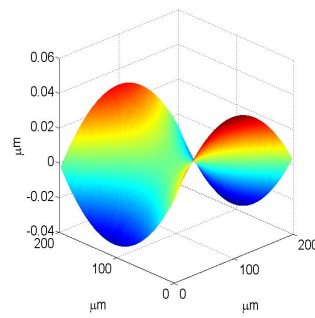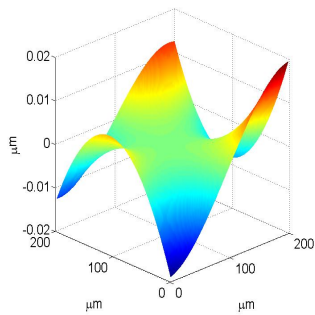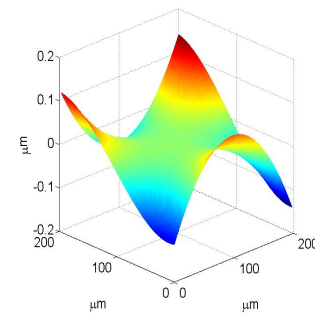Fig. 8. (a) Measured phase distribution and (b) corresponding fitted surface; surface distribution of (c) the focus term, (d) the third order spherical aberration, (e) the astigmatism at 45° term, (f) the astigmatism at 90°, (g) the triangular astigmatism on x base, (h) the triangular astigmatism on y base.

A similar analysis was carried out in case of the *SLR*. At the end of the process, the liquid droplets are clearly separated as showed in Fig.9.
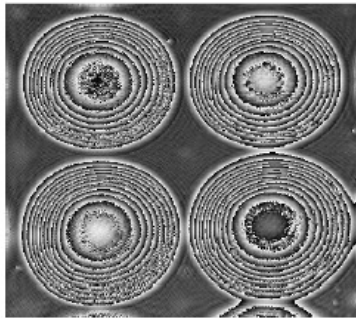

Fig.9 Wrapped phase distribution for lenses in separate like regime

The number of fringes is clearly higher compared to the case of the *WLR* and their density increases from the central to the side region of the lenses. This means that, in case of *SL*, the slope is more pronounced in correspondence of the peripheral regions and that the lenses are relatively flat in the centre.

4. IMAGING PROPERTIES

Fig. 10 shows the imaging capability of the microlens array on a portion of USAF phototarget. The LN substrate, with the microlens array, was positioned over the target and observed under optical microscope. The images in Figs. 10(a)-10(b) were acquired at two different focal planes corresponding to focusing the target through the regions outside and

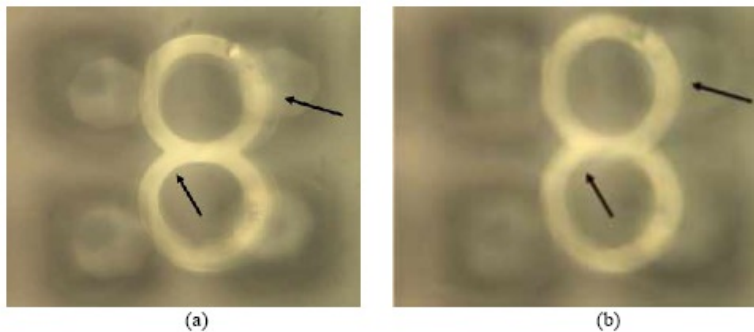inside the aperture of the microlenses, respectively.

Fig. 10. Optical microscope images of the target "8" observed through the microlens array at two different focal planes imaging the target (a) through the region outside the lenses and (b) through the up-right microlens, where the focusing capability of the microlenses is clearly visible.

5. CONCLUSION

The results presented show the tunability properties of liquid microlens arrays activated by an EW effect under an electrode-less configuration. The liquid microlenses are fabricated by manipulating the surface tension of appropriate oil films through the surface charges generated by the pyroelectric effect in PPLN substrates. Two different microlens regimes can be obtained whenever the temperature is controlled accurately. Basically the oil film thickness determines the generation of separated or wave-like lenses which exhibit different optical properties. The accurate interferometric characterization was motivated by the necessity to have information about the properties of the dynamic focusing behaviour but also with the aim at understanding deeper the physics of the phenomenon. The results show that the focal length variation ranges between 16 mm and 1.5 mm and between 30 mm and 10 mm in case of the WLR and the SLR, respectively. An accurate optical investigation of the microlenses has been performed by a DH based technique, in order to characterize the properties of the liquid microlenses in terms of both focal length tunability and optical aberrations.

The tunability of such microlenses could be of great interest to the field of micro-optics thanks to the possibility of achieving focus tuning without moving parts and thus favouring the miniaturization of the optical systems.

REFERENCES

[1]   Dong, L., Agarwal, A. k., David, D. J., Beebe, J. and Jiang, H. , "Adaptive liquid mcrolenses activated by stimuli-responsive hydrogels," Nature 442, 551-554 (2006).
[2]   Berge, B. and Peseux, J. "Variable focal lens controlled by an external voltage: An application of electrowetting," Eur. Phys. J. E 3, 159-163 (2000).
[3]   Commander, L. G., Day, S. E. and Selviah, D. R., "Variable focal length microlenses," Opt. Comm. 17, 157-170 (2000).
[4]   Huang, P. H., Huang, T. C., Sun, Y. T. and Yang, S. Y., "Fabrication of large area resin microlens arrays using gas-assisted ultraviolet embossing," Opt. Express 16, 3041-3048 (2008).
[5]   Pikulin, A., Bityurin, N., Langer, G., Brodoceanu, D. and Bauerle, D. , "Hexagonal structures on metal-coated two-dimensional microlens arrays," Appl. Phys. Lett. 91, 191106 (2007).
[6]   Krogmann, F. , Monch, W. and Zappe, H. , "A MEMS-based variable micro-lens system," J. Opt. A 8, S330-S336 (2006)
[7]   Cheng, C. C., Chang, C. A. and Yeh, J. A., "Variable focus dielectric liquid droplet lens," Opt. Express 14, 4101-4106 (2006)
[8]   Cheng C. C. and Yeh, J. A., "Dielectrically actuated liquid lens," Opt. Express 15, 7140-7145 (2007).
[9]   Chronis, N., Liu, G. L., Jeong, K. H. and Lee, L. P., "Tunable liquid-filled microlens array integrated with microfluidic network," Opt. Express 11, 2370-2378 (2003).
[10] Zhang, D. Y., Justis, N. and Lo, Y. H., "Integrated fluidic adaptive zoom lens," Opt. Lett. 29, 2855-2857 (2004).
[11] Moran, P. M., Dharmatilleke, S., Khaw, A. H., Tan, K.W., Chan, M. L. and Rodriguez, I., "Fluidic lenses with variable focal length," Appl. Phys. Lett. 88, 041120 (2006).
[12] Ren, H., Fox, D., Anderson, P. A., Wu, B. and Wu, S.T., "Tunable-focus liquid lens controlled using a servo motor," Opt. Express 14, 8031-8036 (2006).
[13] Hou, L., Smith, N. and Heikenfeld, J. , "Electrowetting Modulation of Any Flat Optical Film," Appl. Phys. Lett. 90, 251114 (2007).
[14] Smith, N. , Abeysinghe, D. , Heikenfeld, J. and Haus, Agile, J. W. ,"Wide-Angle Beam Steering with Electrowetting Microprisms," Opt. Express 14, 6557 (2006).
[15] Sun, B. , Zhou, K. , Lao, Y. , Cheng, W. and Heikenfeld, J. , "Scalable Fabrication of Electrowetting Pixel Arrays with Self-Assembled Oil Dosing," Appl. Phys. Lett. 91, 011106 (2007).
[16] Kuiper S. and Hendriks, B. H. W. , "Variable- focus liquid lens for miniature cameras," Appl. Phys. Lett. 85, 1128-1130 (2004).
[17] Lin, J. L. , Lee, G. B., Chang, Y. H. and Lien, K. Y., "Model Description of Contact Angles in Electrowetting on Dielectric Layers," Langmuir 22, 484-489 (2006).
[18] Hsieh, W. H. and Chen, J. H., "Lens-Profile Control by Electrowetting Fabrication Technique," IEEE
[19] Grilli, S., Miccio, L., Vespini, V., Finizio, A., De Nicola, S. and Ferraro, P., " Liquid micro lens array activated by selective electrowetting on Lithium Niobate substrate", Opt. Express 26, 8084-8093 (2008).
[20] Miccio, L., Finizio, A., Grilli, S., Vespini, V., Paturzo, M., De Nicola, S., Ferraro, P .,"Tunable liquid micro lens array in electrode less configuration and their accurate characterization by interference microscopy" Opt Express 17, 2487-2499 (2009).